

## The Study of Molecular Structures for New Banana-shaped Liquid Crystals

<sup>1</sup>S. Choi, <sup>2</sup>Y. M. Huang, <sup>2</sup>A. Jákli, <sup>3</sup>T. K. Lim, <sup>4</sup>C. K. Lee and <sup>1</sup>S. T. Shin

<sup>1</sup>Department of Applied Physics, Korea University, Seoul 136, Korea

<sup>2</sup>Liquid Crystal Institute, Kent State University, Kent, OH 44242, USA

<sup>3</sup>Department of Physics, Korea University Seoul 136, Korea

<sup>4</sup>Department of Chemistry, Kyung Sang National University, Kyung Nam 660, Korea

### Abstract

We have studied the phase transition to look for molecular structure by using several different techniques for new banana-shaped liquid crystals shown in Fig. 1. Based on the similarities to recently observed fluoro-containing materials (switching involves layer structure rearrangement, increasing threshold with increasing temperature) for HC sample (where x is H), we assume that the phase C has a triclinic symmetry corresponding to the double tilted  $smC_G$  phase. The observation that the polarization peak appears at lower field ( $E_o \sim 15V/\mu m$ ) than the amplitude of the threshold ( $E_{th}$ ) can be explained assuming a field induced  $SmC_G$  -  $SmCP$  (or  $SmAP$ ) transition at  $E_{th}$ .

### 1. Introduction

Ferro- and antiferroelectric liquid crystal materials composed of achiral molecules has been recently attracted with increasing attention [1,2]. These developments can be traced back, at least in part, to the prediction that suitably bent achiral molecules (banana-shaped molecules) arranged on smectic layers on average parallel to their bend direction could form a fluid biaxial smectic phase with a macroscopic polarization in the smectic layer planes:  $C_P$  [1,2].

$SmC_G$  is a biaxial smectic phase [3]. In Smectic  $C_G$  phase all three principle axes include an angle with the smectic layers different from  $0^\circ$  and  $90^\circ$  (double tilted structure). As a result, Smectic  $C_G$  phase has, global  $C_1$  symmetry, the lowest possible symmetry: triclinic [4].  $C_1$  symmetry means that this phase has no symmetry, at all and that therefore a macroscopic polarization exists.

In this paper, we study the status of switching in various phases that  $SmC_G$  phase can not be switched by induced fields, but  $SmCP$  and  $SmAP$  phases can be.

We also discuss the voltage dependences of the switching, and the switching mechanisms by various techniques.

### 2. Experimental Details

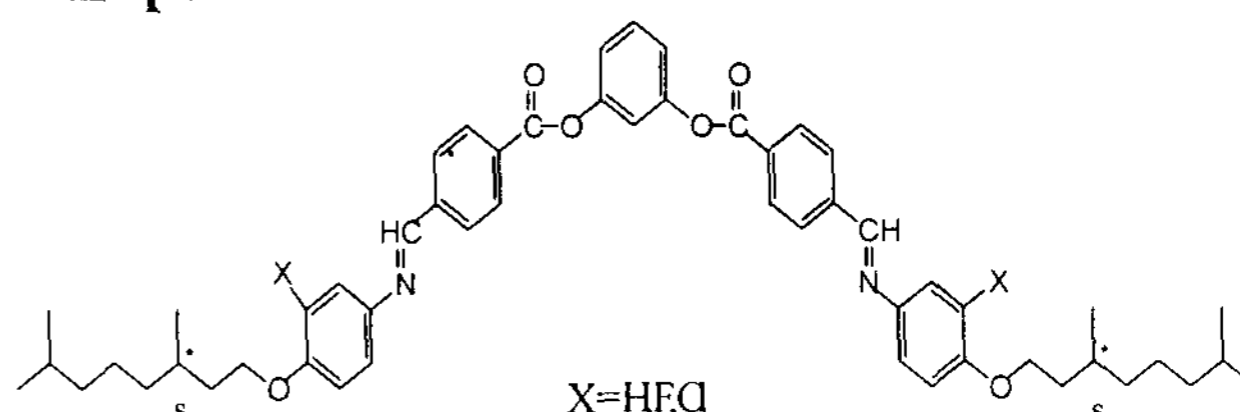


Figure 1. Molecular structures of the three banana-shaped molecules. X=H, F, Cl : 1,3-phenylene bis [4-[4-{4-(3(S),7-dimethyloctanyloxy)}phenyliminomethyl]benzoate].

We studied films filled in  $4\mu m$  Displaytech cells with antiparallel rubbed polyimide layers. The samples were placed in INSTEC HS200 heat stage that allows regulation of the temperature with the precision of  $0.1^\circ C$ .

### 3. Results and discussions

#### 3.1 Textural observations

*On cooling* the phase C appears in the isotropic phase in form of helical filaments that are the hallmarks of the  $B_7$  phase (see Figure 2/a). The helical structures also indicate that the phase is chiral. Applying electric fields under cooling during the transition the filaments become deformed and often ribbon and fan-shaped domain formed and the extinction crosses of these domains rotate with the periodicity of the electric fields (see Figure 3/b and c). The amplitude of the rotation angle is basically proportional to the magnitude of the electric field reaching about  $20$  degrees at  $E \sim 15V/\mu m$ .

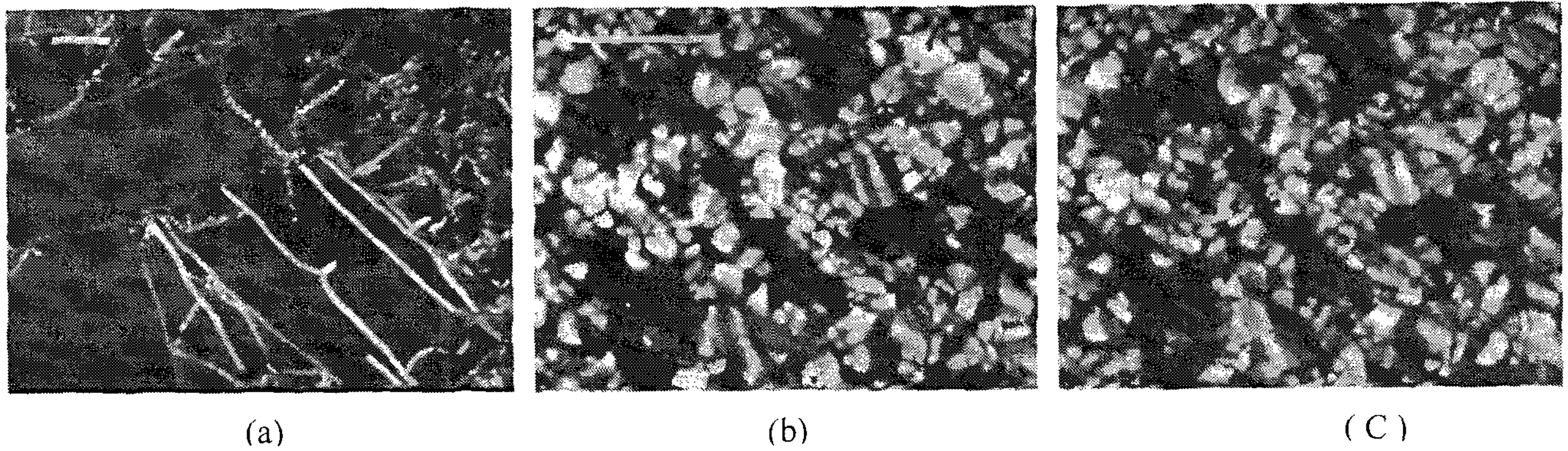


Figure 2. Textures at 110°C under (a)  $E_{peak}=+30V/\mu m$ , (b)  $E=0$ , and (c)  $E_{peak}=-30V/\mu m$  fields. Bars indicate 100 $\mu m$ .

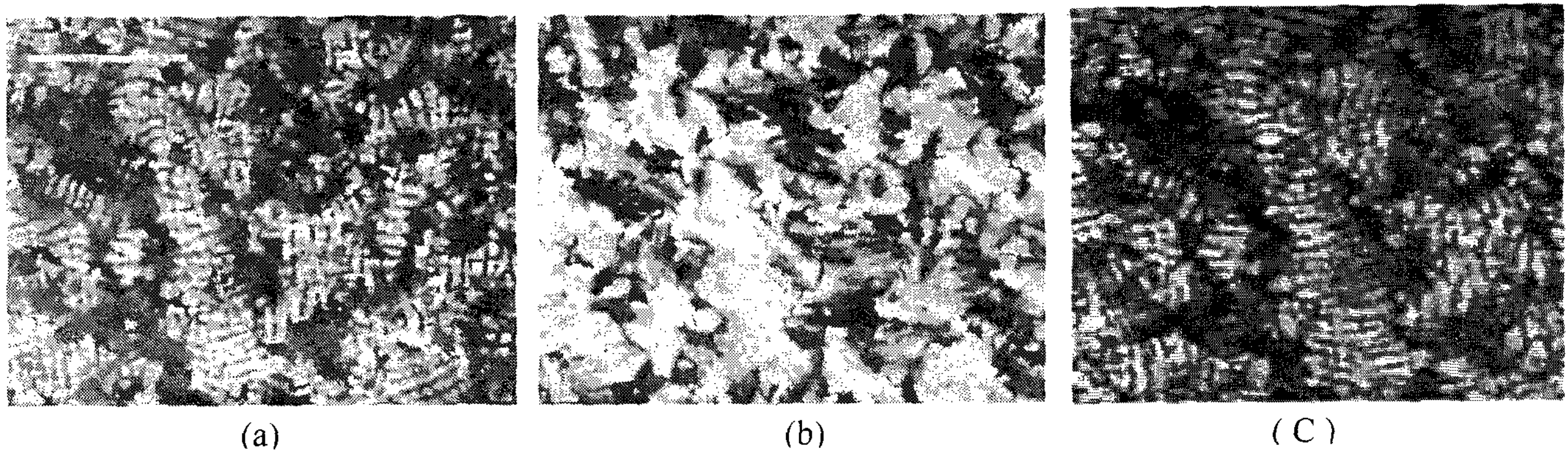


Figure 3. Textures of HC at 120°C on cooling from the isotropic phase (black area). (a) formation of helical filaments at  $E=0$ ; Fan-shape and ribbon-like textures under  $E=+1V/\mu m$  and (b)  $E=-1V/\mu m$  field. Bars indicate 100 $\mu m$  lengths.

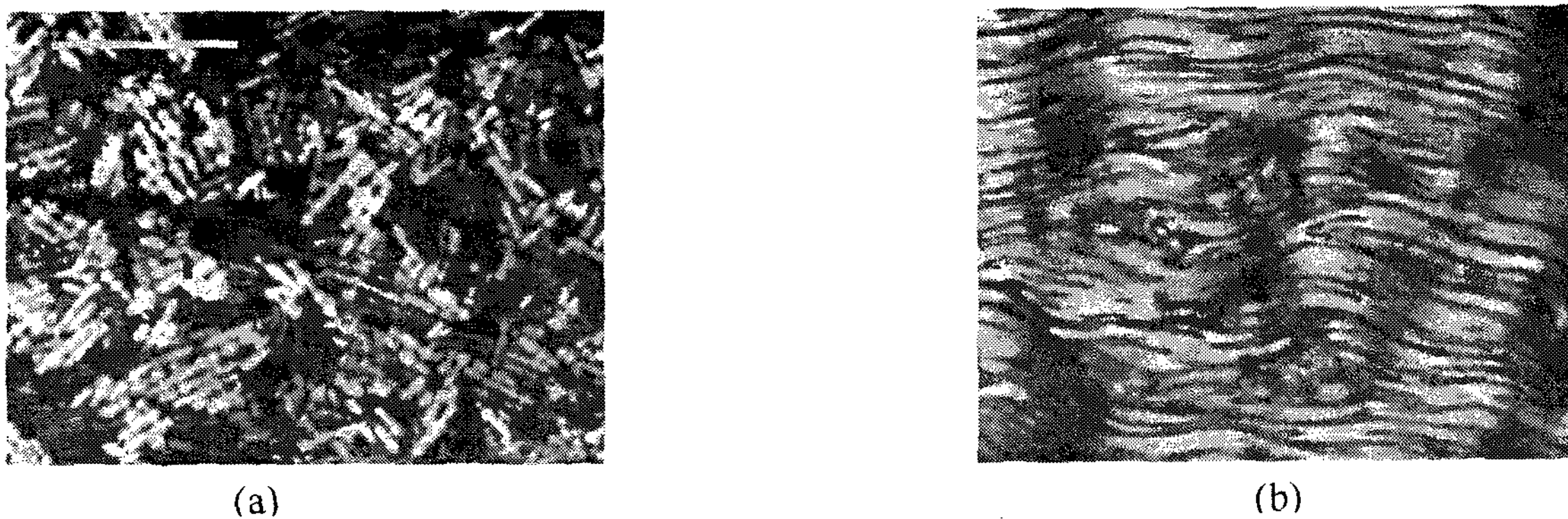


Figure 4. Textures under electric field of  $E_{rms}=16V/\mu m$ . (a)  $T=117^\circ C$ ,  $f=1Hz$  square-wave field and (b)  $T=110^\circ C$ ,  $f=54Hz$ , triangular wave field. Bars indicate 100 $\mu m$  lengths.

The textures above  $E_{th} \sim 30V/\mu m$  fields are not sensitive to the sign of the electric field [Figure 3. (a) and (c)] and are characterized by a higher (green) birefringence color. This might indicate racemic -type switching, i.e. the textures under positive and negative fields look alike. This is especially interesting, since the appearance of helical filaments and the rotation of the extinction directions at lower fields indicate chiral structure. Turning off the field from this site the

original texture with yellow birefringence color appears gradually in about 1-2 sec [see Figure 3 (b)].

Under rectangular fields the texture breaks up to small stick-like domains [see Fig. 4 (a)] and the switching is accompanied by mechanical rotations of the sticks. At lower temperatures – especially at higher frequencies – the texture becomes smoother and vivid flow effects are observed as shown in Fig. 5 (b).

### 3.2 Conductivity

We measured the DC conductivity of the material both in heating and cooling with 1 °C/min rate and plotted in Figure 5. We observed that the phases appeared below the isotropic liquid I are different in cooling and heating. The phase appeared in cooling will be designated as C and the one appeared in heating will be called H. The monotropic C phase has an activation energy  $E_a(C) = 22.7 \text{ kcal/mol}$  and transfers to the lower temperature solid phase S at  $T_{C-S} = 102^\circ\text{C}$ . The phase S has an activation energy  $E_a(S) = 12 \text{ kcal/mol}$ . In heating, H appears at  $T_{S-H} \sim 92^\circ\text{C}$ . The activation energy of H is  $E_a(H) = 18.8 \text{ kcal/mol}$ , i.e. it is smaller than of the phase C. The H-I transition temperature is  $T_{H-I} \sim 122^\circ\text{C}$ , slightly larger than the I-C transition, which is  $T_{I-C} \sim 119^\circ\text{C}$ . The activation energy of the isotropic phase is:  $E_a(I) = 12 \text{ kcal/mol}$ .

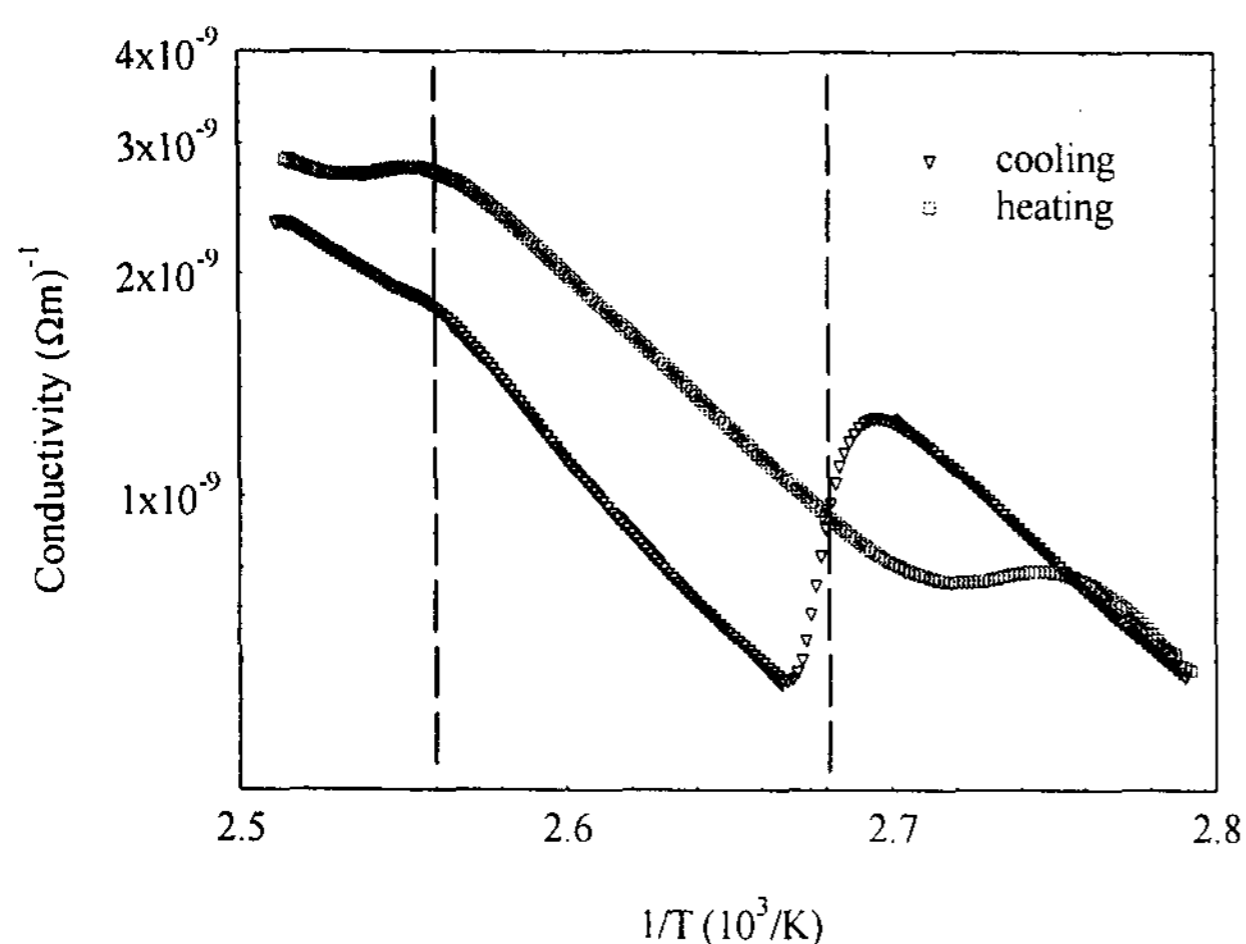


Figure 5. Conductivity as a function of temperature in heating and in cooling. Interesting results are that the mesophase in heating has different conductivity and slightly different activation energies. This indicates different structures in heating and cooling.

### 3.3 Polarization current measurements

Near the transition ( $>119^\circ\text{C}$ ), no polarization peaks could be observed up to  $40 \text{ V}/\mu\text{m}$  triangular fields. At decreasing temperatures, however a clear polarization peak appears in each half period above  $E_{th}$  indicating ferroelectricity. It is important to note that  $E_{th}$  is increasing with increasing temperatures;  $E_{th}(110^\circ\text{C}) = 27 \text{ V}/\mu\text{m}$ ,  $E_{th}(118^\circ\text{C}) = 32 \text{ V}/\mu\text{m}$ , and  $E_{th}(119^\circ\text{C}) = 38 \text{ V}/\mu\text{m}$ . Similar behavior was observed recently both in asymmetric[5] and symmetric fluoro-containing banana-shaped liquid crystals.

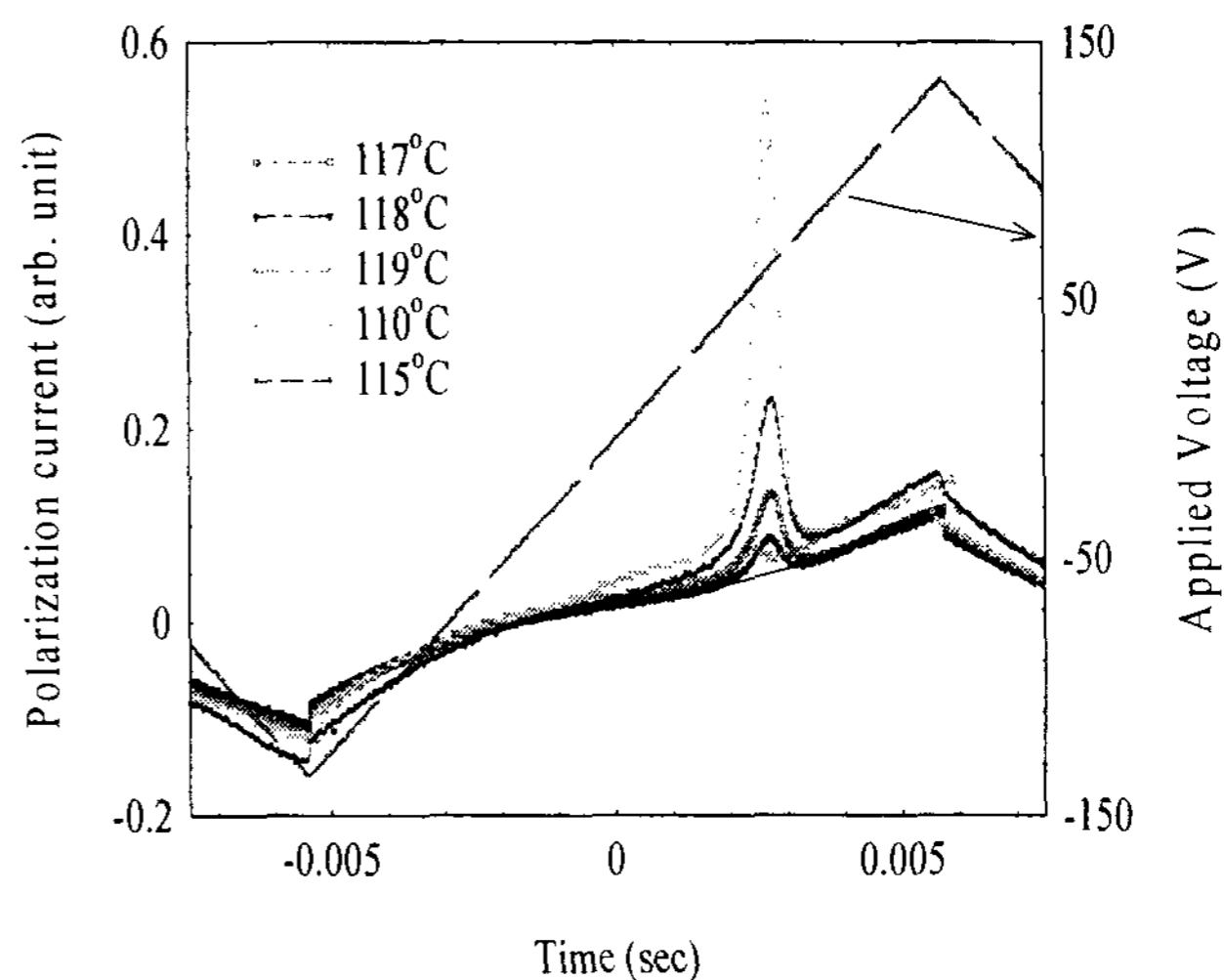


Figure 6. Time dependence of the switching current under triangular voltages at different temperatures. The polarization calculated from the area above the baseline corresponds to  $P_s = 250 \text{ nC/cm}^2$ .

Interesting note is that the polarization peak appears only when the amplitudes of the triangular fields exceed  $E_{th} \sim 25 \text{ V}/\mu\text{m}$ , but the polarization peak appears at much lower values,  $E_o \sim 15 \text{ V}/\mu\text{m}$ .

The polarization switching times were measured under square-wave fields. The time dependences of the polarization current curves for several temperatures are shown in Figure 7.

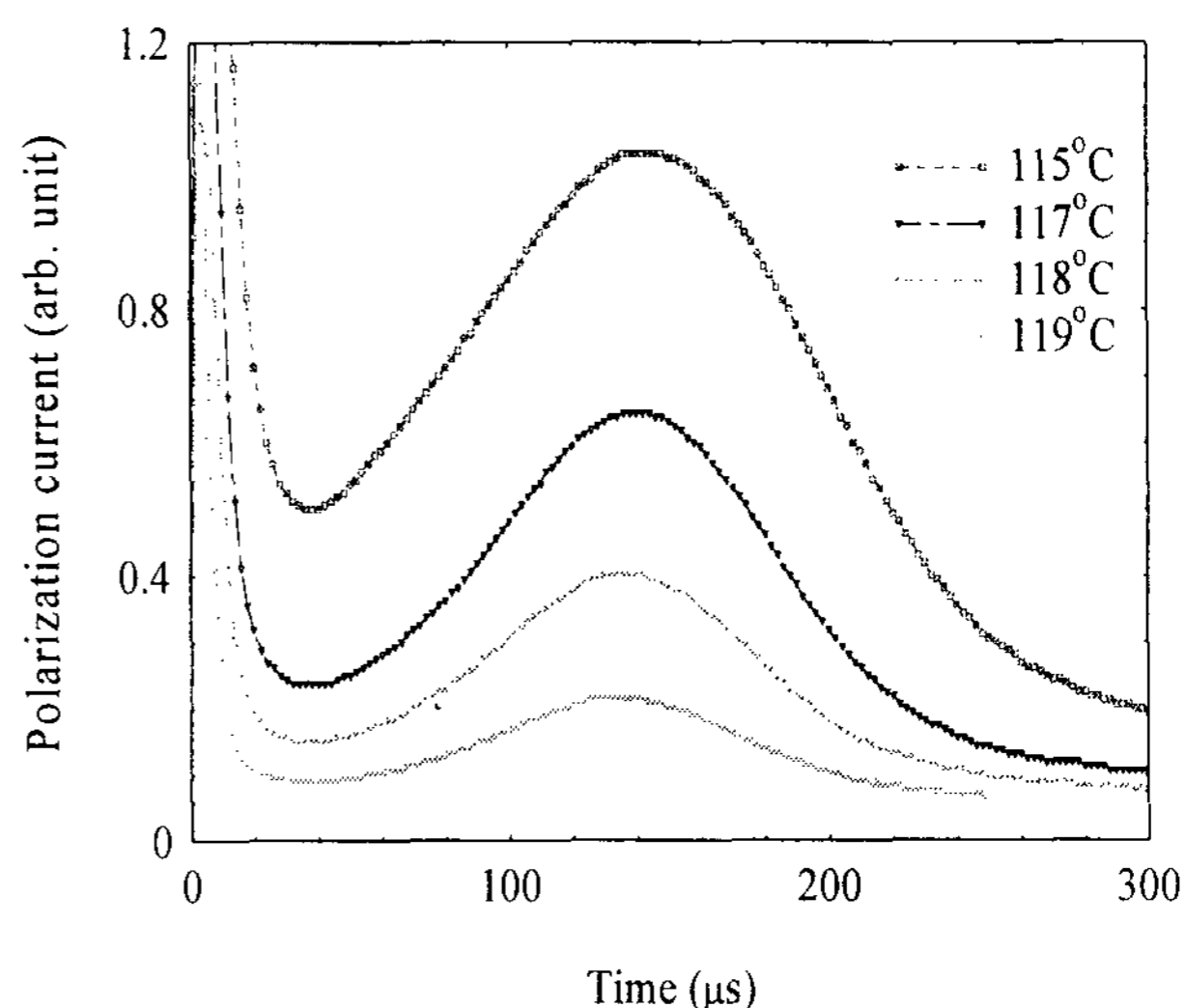


Figure 7. Polarization current under step-wise field reversal ( $E = 16 \text{ V}/\mu\text{m}$ ).

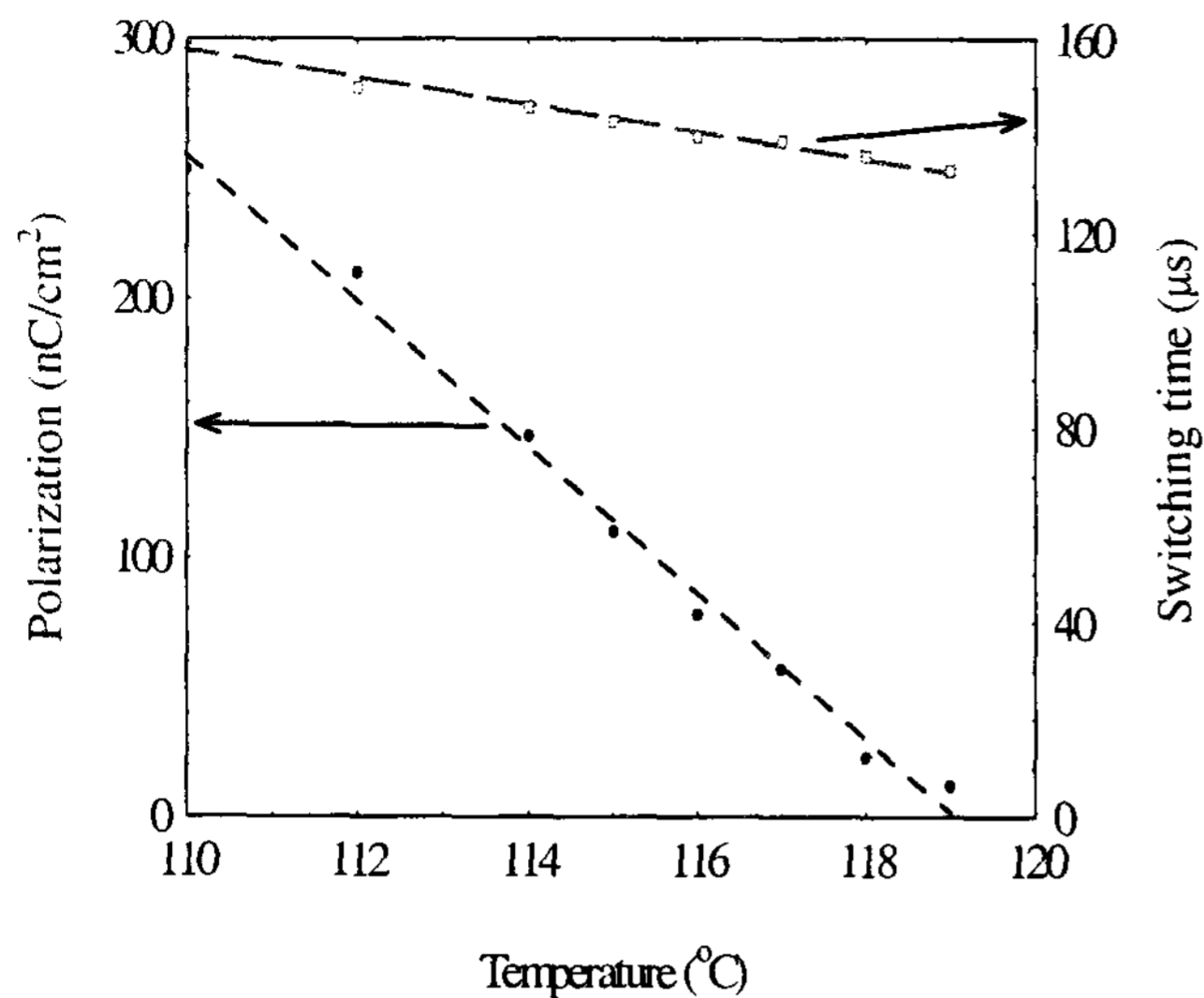


Figure 8. Polarization and switching time as a function of temperature.

The temperature dependences of the polarization and the switching time are depicted in Fig. 1. It can be seen that both of the magnitude of the polarization and the switching time decreases proportional to the increasing temperature.

Here we have to note that in the off state the phase C was stable at least for hours, but under  $E > E_{th}$  fields and at lower temperatures (below 112°C) the material freezes in a few minutes. The texture of the frozen-out phase [see Fig. 9 (a)] is not switchable at least up to the limit of our experimental possibilities ( $E \sim 45 \text{ V}/\mu\text{m}$ ).

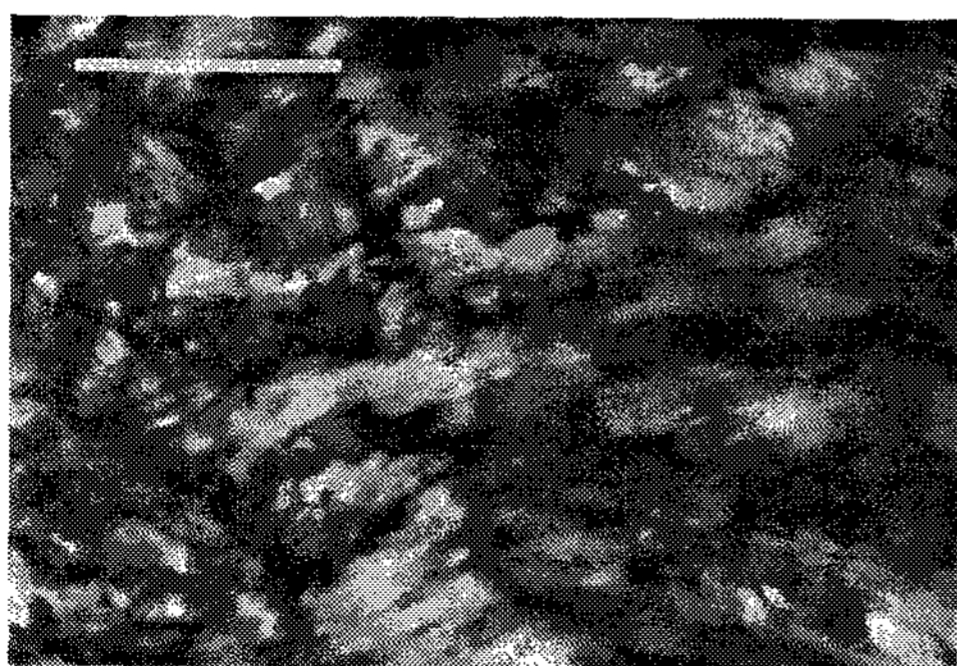
In heating from the phase S, the structure looks similar to the frozen out phase and could not be switched up to  $45 \text{ V}/\mu\text{m}$  fields. It is also remarkable that phase H melts to I forming threads similar to the structures when the frozen out phase was melted [see Fig. 9 (b)].

### 3.4 Dielectric constant measurement

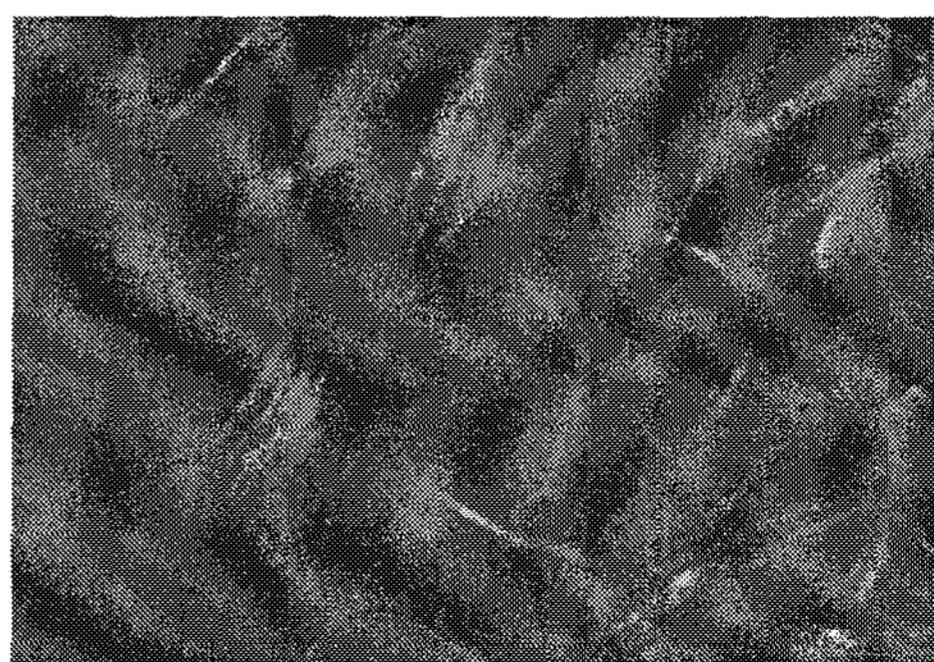
We prepared the  $3.0 \mu\text{m}$  thick cell of the anti-parallel rubbed homogeneous samples. For the homogeneous cells, RN1199 polyimide made by Nissan Chemicals was used, which has  $1.1^\circ$  low pretilt angle. The values of capacitance for dielectric constant and resistance for dielectric loss (imaginary part of dielectric constant) were measured by using HP4284 LCR meter. The real and imaginary dielectric constants were calculated. [See Fig. 10] The real and imaginary dielectric constants,  $\epsilon'$  and  $\epsilon''$ , were measured in the frequency range between 20Hz and 1MHz while temperature was changed in  $1^\circ\text{C}/\text{min}$  cooling, controlled by a temperature control unit (Instec STC 200) within  $\pm 0.1^\circ\text{C}$ .

The dielectric constant increases steeply at the banana phase ( $B_7$ ) phase transition temperature, and then it decreases with stabilize crystal.

Relaxation Frequency is 400KHz. it is higher than frequency of relaxation frequency mode [See Fig. 11]. The higher frequency mode is not clarified. It might be assigned to a rotation around the molecular shot axis.



(a)



(b)

Figure 9. Texture after phase C was frozen out under high fields; (a) at  $T=110^\circ\text{C}$  and (b) upon the transition to the isotropic phase. Bar indicates  $100 \mu\text{m}$  lengths.

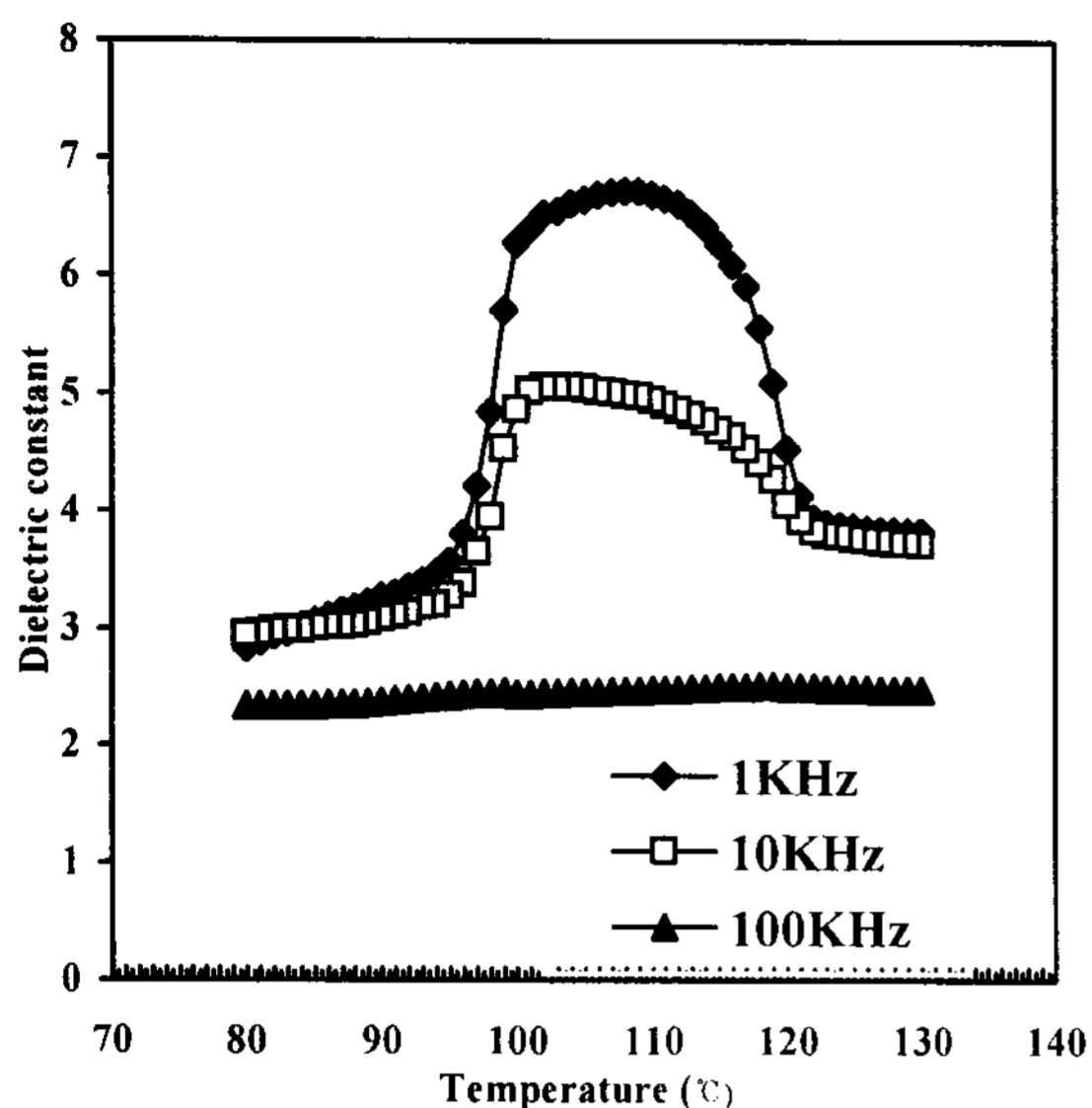


Figure 10. Temperature dependence of the dielectric constant for 3  $\mu\text{m}$  cell gap sample.

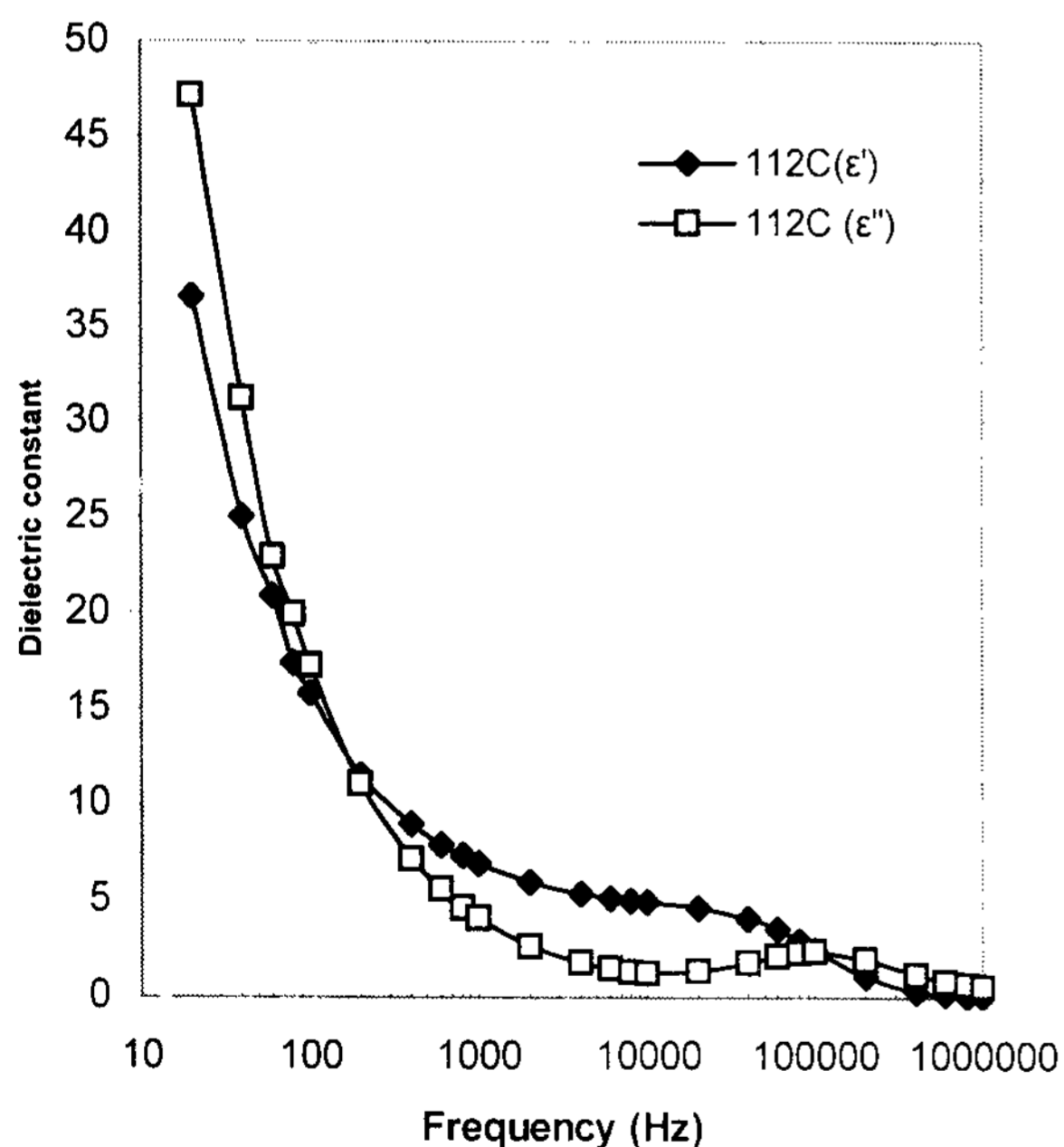


Figure 11. Frequency dependence of the real and imaginary dielectric constants.

The higher frequency mode is not considered to be the Goldstone mode. Due to the low viscosity, the result of spontaneous polarization is similar to the result taken in low frequency mode.

#### 4. Conclusions

Based on the similarities to recently observed fluoro-containing materials, we assume that the phase C has a triclinic symmetry corresponding to the double tilted  $\text{SmC}_G$  phase. The observation that the polarization peak appears at lower fields ( $E_0 \sim 15 \text{V}/\mu\text{m}$ ) than the amplitude of the threshold ( $E_{\text{th}}$ ) can be explained assuming a field induced  $\text{SmC}_G$ - $\text{SmCP}$  (or  $\text{SmAP}$ ) transition at  $E_{\text{th}}$ . We think that the polarization cannot be switched in the  $\text{SmC}_G$  phase, but only in the field-induced  $\text{SmCP}$  or  $\text{SmAP}$  phase, where the switching threshold is smaller than the threshold for the field-induced phase transition. X-ray measurements carried out in electric fields may verify this assumption (these will not be easy due to the very high field needed). X-ray measurements will be needed also to clarify the structures of the mesophases formed in heating and cooling.

#### 5. References

- [1] H. R. Brand, P. E. Cladis, and H. Pleiner, *Macromol.* **25**, 7233 (1992).
- [2] P. E. Cladis and H. R. Brand, *Liq. Cryst.* **14**, 1327 (1993)
- [3] P. G. De Gennes, *The Physics of Liquid Crystals*, Clarendon Press, Oxford, (1975).
- [4] H. R. Brand, H. Pleiner, *J. Phy. II France* **1**, 1455 (1991).
- [5] S. Rauch, P. Bault, H. Sawade, G. Heppke, and A. Jáklí, *Phys. Rev. E*, **66**, 021706, (2002).